

CORROSION TESTS IN THE STATIC CONDITION AND INSTALLATION OF CORROSION LOOP AT KAERI FOR LEAD-BISMUTH EUTECTIC

J-E. Cha, C-H. Cho, T-Y. Song

Korea Atomic Energy Research Institute, Korea

Abstract

Lead-bismuth eutectic (LBE) corrosion has been considered as an important design factor to limit the temperature and velocity of the accelerator-driven transmutation system. For the corrosion study, KAERI finished the set-up of the LBE static corrosion facility and also finished the preliminary design of a dynamic corrosion loop and started a set-up process to construct the loop by the fall of 2004. In this paper, we describe the results of the preliminary static test during 500 hrs under a reduced condition to check the performance of the static facility. We also describe a design concept of corrosion loop and the state of the art for its installation at KAERI, as well as the results of EM pump preliminary testing.

Introduction

ADS has been widely studied over the past few years, as it has the possibility to transmute minor actinides and long-lived fission products in nuclear spent fuel. Since 1997, KAERI has also conducted systematic studies to develop the ADS system, called HYPER [1]. HYPER is a 1 000 MWth fast spectrum reactor with $k_{\text{eff}} = 0.98$ that has been designed to transmute TRU, ^{99}Tc and ^{129}I . LBE is preferred as the target material due to its high production rate of neutrons and effective heat removal. Recently, LBE has been widely studied as a core coolant and target material of ADS in various countries. However, LBE and lead are more corrosive than sodium because the solubility of Ni, Cr and Fe is high. Thus, LBE corrosion has been considered as an important design factor to limit the temperature and velocity of the ADS system [2-4].

In designing HYPER, it was taken into consideration that the average temperatures of LBE at the inlet and outlet are 340 C and 490 C, respectively. The maximum temperature of the cladding is estimated at around 575 C. In the case of the beam window, the LBE corrosion effect can be combined with radiation damage to produce more severe damage. The maximum temperature of the beam window contacted with LBE is designed not to exceed 500 C.

Several methods have been considered to prevent the corrosion problem in LBE. In the research on LBE technology, it has been made clear that the corrosion behaviour is controlled by the oxygen concentration in the liquid LBE. Thus, one method is to form a stable oxide layer on the material surface through an oxygen level control in LBE. Another is to modify the material compositions or the surface of the material. If an appropriate method to prevent corrosion cannot be found, the design should be modified so that the maximum temperature decreases.

Static corrosion tests are useful to investigate the corrosion properties and modes of various kinds of materials to develop corrosion-resistant materials for liquid LBE. KAERI recently finished the set-up of the LBE static corrosion facility and began a static test and systematic research to develop the measuring techniques for the control of the oxygen concentration.

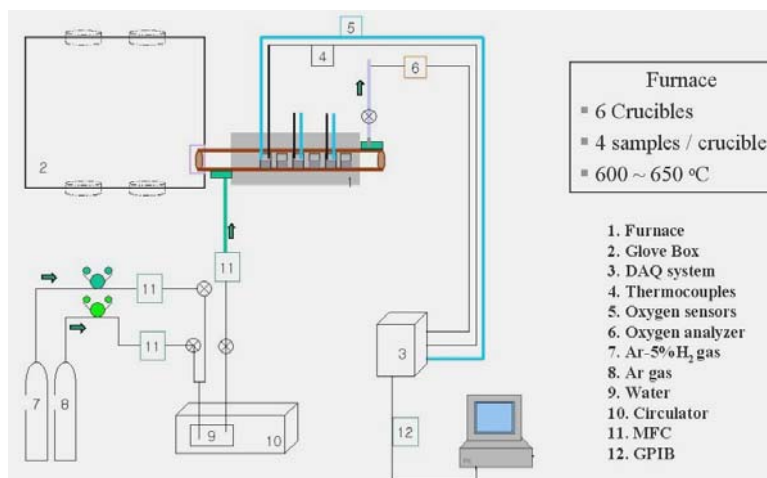
Corrosion tests using a liquid-metal loop are also necessary to estimate the corrosion and erosion behaviour in the LBE flow. KAERI recently finished the preliminary design of a dynamic corrosion loop and started a set-up process to construct the loop by the fall of 2004. We also have a long-term plan to build a proton irradiation test loop since it is essential to estimate the effects for irradiation of high-energy protons and neutrons on the beam window materials. In this paper, we described the results of the preliminary static test with SUS316 and HT9 during 500 hrs under a reduced condition to check the performance of the static facility. For the corrosion loop, we describe a general design concept and the state of the art for the installation at KAERI.

Test in static corrosion facility

Figure 1 shows the schematics of the static corrosion facility recently installed at KAERI. It is mainly composed of tube furnaces, a gas supply system and a glove box. The glove box was installed to control the gas concentration during the treatment of test samples. A wall of the glove box is connected to a flange of the furnace to install and draw out the test samples for the static corrosion experiment; bottom of the glove box is also connected with a flange of the test section of the dynamic corrosion loop.

The gas control of the glove box is conducted with an argon gas or a mixture gas of argon and hydrogen. The furnace has three independent heaters to reduce the temperature difference along the quartz test tube (70 mm in inner diameter and 700 mm in length). The gas concentration of the furnace

Figure 1. Schematics of static corrosion facility



is monitored at the inlet and outlet position with the oxygen analysing system of ZIROX SMGT 1.6 up to oxygen partial pressure $O_2(10^{-1})$ ppm. The temperature of liquid LBE is measured by a K-type sheathed thermocouple in each crucible. The mass flow of gas is controlled with the mass flow controllers (MFC), the pressure regulators and the needle valves.

A total of six crucibles are installed in the test tube of the furnace and a total of four samples are mounted in each crucible. The LBE mass in a ceramic crucible was around a total of 55 g LBE for the corrosion test, which was calculated by considering the solubility, the volume of LBE and the contact surface between the samples and the LBE. The test samples in Table 1 were prepared by annealing for one hour at 1 050 C. The heat treatment was conducted at 750 C for two hours for the HT9 after annealing. Its dimensions are: 10 mm in width, 18 mm in height and 2 mm in thickness. The experiment was conducted at a temperature of 650 C during 500 hours. The oxygen concentration was controlled with the mixture ratio of H_2 and H_2O vapour.

Table 1. Chemical composition of specimens (wt.%)

Material	C	Si	Mn	Ni	Cr	Mo	V	Nb	W	P	S	N
HT9	0.19	0.36	0.59	0.53	11.79	0.99	0.31	0.02	0.49	0.019	0.006	< 0.01
316L	0.02	0.35	1.8	12.1	17.3	2.31	–	–	–			

Figure 2 shows the EPMA results of the 316L and HT9 exposed to LBE at 650 C with a reduced condition for 500 hours. The oxygen meter shows that the oxygen content in the flowing gas is less than 10^{-8} wt.%. Table 2 explains the EPMA data results of Figure 2. In spite of the well-known serious corrosion attack for 316L, no dissolution attack was shown and the oxygen layer was not detected. It is necessary for us to investigate the test conditions, which should include the oxygen concentration and the surface of the specimens.

Corrosion loop

Figure 3 shows the schematic diagram of the dynamic corrosion loop to be installed at KAERI. The LBE loop is an isothermal loop. The flow velocity in the test section was designed to be around 2 m/s in the range of 400-550 C and the charging volume of the LBE is around 0.03 m^3 in the circulation loop.

Figure 2. SUS 316L, HT9 at 650 C with oxygen content $<10^{-8}$ wt.%(500 hrs)

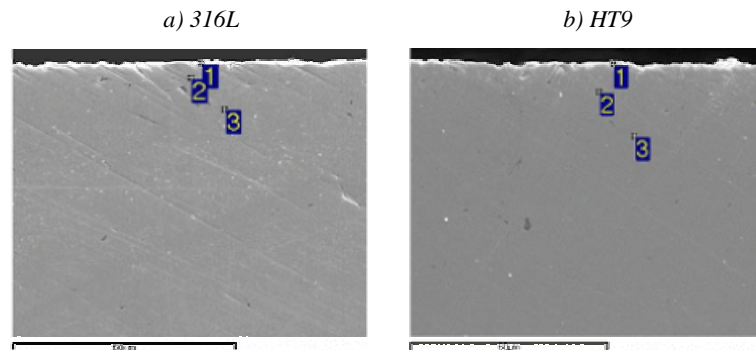
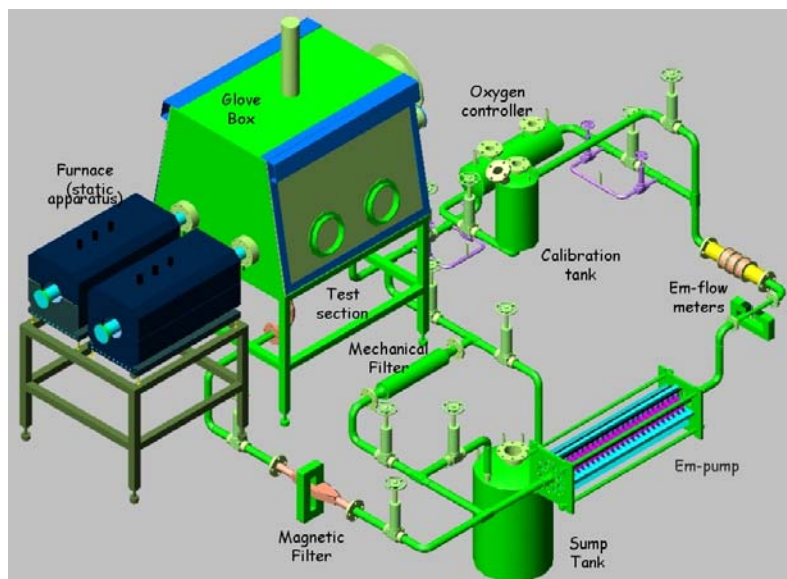


Table 2. The EPMA results of 316L, HT-9 at 650 C

Location	316L						HT9					
	Fe	Cr	Ni	Pb	Bi	O	Fe	Cr	Ni	Pb	Bi	O
1	67.43	21.13	9.98	0.25	0	1.20	93.27	3.87	0	0	1.33	1.54
2	70.76	17.48	10.62	0	0.42	0.72	91.27	6.26	0.16	0	1.56	0.75
3	70.08	17.25	10.83	0	0.95	0.88	85.12	12.15	0.51	0	1.42	0.81
Original	70.6	17.3	12.1				87.68	11.79	0.53			

Figure 3. Three-dimensional schematics of corrosion loop



The LBE loop is mainly composed of a main test loop, a bypass loop for filtering LBE and a mixture gas supplying system. The liquid metal in the main test loop circulates in the following order: EM pump fi EM flow meter fi oxygen controller fi test section fi magnetic filter fi EM pump. The major specifications of KAERI's loop are summarised in Table 3.

Since LBE is a heavy liquid metal and has a higher viscosity than water or sodium, the forced convection loop should be designed to reduce the pressure drop to be as small as possible and adopt a pump with a high pumping head. From the analysis of the pressure drop, the specification of the piping

Table 3. Major specification of corrosion loop

Operation temperature	400 C ~ 550 C (max. 600 C)
Liquid metal volume	Pb 44.5%, Bi 55.5%, 0.08 m ³
Test section	3/4 inch, Sch. 40, SUS 316 seamless pipe, $V_{\text{mean}} = 2$ m/s (at 45 lpm)
Sample specification	φ 8 mm, thickness 2 mm, height 5 mm
Piping system	1.5 inch, Schedule 40, SUS 316 pipe
Flow measurement	EM flow meters
Liquid metal pumping	EM pump (60 lpm, 4 bar, 40 kVA)
Oxygen control	H ₂ /H ₂ O partial pressure (10 ⁻⁵ wt.% ~ 10 ⁻⁷ wt.%)
Purification	Magnetic filter, mechanical filter

system was determined as 1.5-inch pipe to reduce the pressure drop by a high mean fluid velocity. The pressure drop of the main test loop was estimated at around 3 bar (3 m head in LBE) with a flow rate of 60 lpm.

The LBE is circulated with an electromagnetic pump (60 lpm, 4 bar, 40 kVA), which is a kind of annular linear induction pump designed by an equivalent electric-circuit method. By considering the uncertainty, the pump head was conservatively determined as 4 bar under a maximum flow rate to overcome the pressure loss of the LBE flow.

The flow rate is measured with electromagnetic flow meters based on Faraday's induction law [5]. In the present study, several types of electromagnetic flow meters will be serially installed to investigate the effects such as contact impedance due to wall oxidation and others. The performance of every EM flow meter can be calibrated with a calibration tank in the loop.

A total of 0.08 m³ of LBE is stored in the sump tank before charging into the test loop. Most parts of the piping system are made of stainless steel pipe 1.5 inches in inner diameter (SUS 316, 1.5 inch schedule 40) and are connected by welding for the prevention of leakage of the LBE.

The oxygen concentration of the range of 10⁻⁷ wt.% ~ 10⁻⁵ wt.% is controlled by a chemical equilibrium between the mixture gas of hydrogen-argon and the water vapour. At present, the oxygen concentration in the LBE and mixture gas is measured with an oxygen sensor made of a yttria-stabilised zirconia as a solid electrolyte cell and Pt/air as a reference system. The electric potential between the LBE flow and the reference electrode is measured by a voltmeter with a high input impedance to maintain the difference of the oxygen concentration. The oxygen partial pressure is determined by Nernst's equation.

The oxygen controller is used to control the level of the oxygen concentration in the loop and expand the liquid LBE during the test. Direct control of the oxygen concentration is not easy since the required oxygen level is very low. However, the oxygen partial pressure P_{O_2} can be chemically controlled with the ratio of the other gases involved, e.g. the H₂/O₂/H₂O. In order to control the oxygen level in the loop, a mixture gas of argon, hydrogen and water vapour is continuously injected into the LBE flow in the oxygen controller.

$$C_o = C_{o,s} \left(\frac{P_{O_2}}{P_{O_2,s}} \right)^2 \quad [\text{wt}\%] \quad (1)$$

$$P_{O_2} = \left(\frac{P_{H_2O}}{P_{H_2}} \right)^2 \exp \left(\frac{2DG_{H_2O}^{\circ}}{RT} \right) \text{ [bar]} \quad (2)$$

where C_O is the oxygen concentration, $C_{O,s}$ is the solubility of oxygen in the LBE and P_{H_2O} and P_{H_2} are the partial pressure of H_2O and H_2 , respectively and $DG_{H_2O}^{\circ}$ is the oxygen potential of water vapor.

Test samples are installed in the test section with an annular cross-section. In order to treat the test samples in a regulated oxygen environment, the upper part of the test section is installed inside the glove box. The test section is made of a seamless pipe (SUS 316, 3/4 inch, Schedule 40). Most LBE flows in the test section have to be turbulence due to a high density. Test samples are mounted from a distance of 15~20 D_h (hydraulic diameter of test section). In fact, the distance of the entrance zone is longer than this distance. However, we determined the distance as small as possible by considering the pressure drop, the static head and the height of set-up space. Test samples in Table 4 will be firstly prepared from the static test and have the dimension of 8 mm in outer diameter, 2 mm in thickness and 5 mm in height.

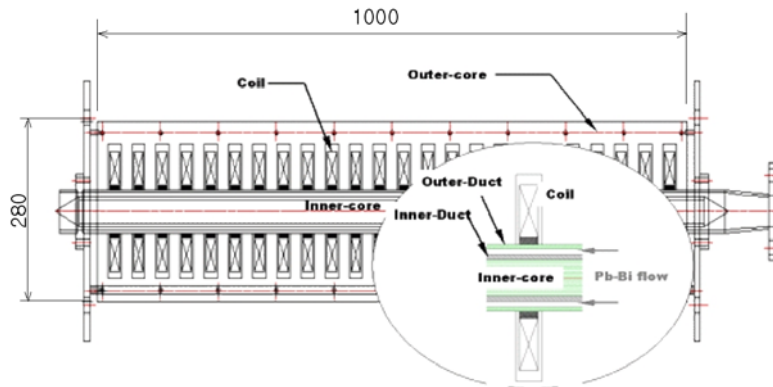
Table 4. Compositions of test samples (composition, wt.%)

	C	Si	Mn	Ni	Cr	Mo	V	Nb	W	P	S	N
HT9	0.19	0.36	0.59	0.53	11.79	0.99	0.31	0.02	0.49	0.019	0.006	0.01
HT9M	0.145	0.1	0.45	0.46	9.79	1.23	0.2	0.18	–	<0.003	<0.003	0.02
HT9MN	0.15	0.072	0.49	0.05	10.0	1.28	0.205	0.204	–	0.002	0.004	>0.02
T91	0.105	0.43	0.38	0.13	8.26	0.95	0.20	0.075	–	0.009	0.003	0.055
9Cr-1Mo	0.099	0.32	0.42	0.10	9.03	0.96	0.22	0.094	–	<0.003	0.003	0.032
316LN	0.022	0.53	0.87	10.6	17.69	2.61	–	–	–	0.02	0.001	>316ss
AISI 316L	0.02	0.35	1.8	12.1	17.3	2.31	–	–	–			
9Cr-2WVTa	0.11	0.21	0.44	<0.01	8.90	0.01	0.23	–	2.01	0.015	0.008	0.0215

Generally, an EM pump has been employed to circulate electrically conductive liquids like molten metals by Lorentz force ($J \cdot B$) generated from the surrounding magnetic field and its perpendicular current. We adopted an EM pump as the pumping device in the test loop by considering corrosion. In the present design, the EM pump of an annular linear induction type with a flow rate of 60 lpm and a head of 4 bar is designed by using the electrical equivalent circuit method that is applied to linear induction machines for the circulation of the liquid LBE. In an annular-type pump, the developing force is generated by a cross product of the azimuthally-induced current (J) at the liquid metal and the radial magnetic field (B) from the outer core. The maximum velocity was 1.5 m/s in the annular channel of the EM pump.

Figure 4 shows the cross-section of the annular linear induction EM pump to be designed. It is divided into the electromagnet made of the inner and outer cores with a high magnetic permeability and exciting conductor coils, and ducts with a narrow annular channel gap for the liquid-metal flow. The EM pump with designed variables by the equivalent circuit method is operated for the corrosive LBE circulation under a high temperature around 500 C. Therefore, the material of the EM pump should be compatible with those operation conditions. A silicon-iron sheet (0.35 mm) with a high magnetic permeability is selected as the core material to keep the magnetic property under a high temperature. The outer and inner cores are fabricated by the stacking of thin silicon-iron plates to reduce the Joule's heat losses by the eddy current. Moreover, cores are arranged radially so that the stacked direction of the inner core is consistent with that of the outer core for directing the strong magnetic field towards

Figure 4. Schematics of annular linear induction EM pump



the radial direction. As coil conductors, an alumina-dispersed, strengthened copper band (GLIDCOP, AL-15, 1.0 mm) is employed taking into account the mechanical and electrical properties under a high temperature, which are a small volume expansion coefficient and a sufficient electrical conductivity compared with the other conductors in the operation environment. The mica-silicon insulator (1.0 mm, SR864G) that has flexibility in the coil curvature and durability under high temperatures is inserted between the coils to prevent an electrical short circuit. On the other hand, to prevent the distortion of the magnetic field at the narrow flow channel, the ducts are made of austenitic stainless steel with non-ferromagnetic material.

Figure 5 shows an EM pump system manufactured for the corrosion loop and a measuring system to investigate its performance. The performance of the EM pump was measured using a one-component dynamometer and strain amplifier after calibration with the known weight. For the verification of the magnetic field, we used a three-component Gauss meter and a transverse and an axial-type probe. The EM pump and dynamometer were installed on the accurate stone table to prevent vibration and deformation. A stainless steel pipe was inserted into the annular space as an LEB simulator and several thermocouples were attached to check the temperature of the EM pump.

Figure 5. EM pump system and the measuring system of its performance

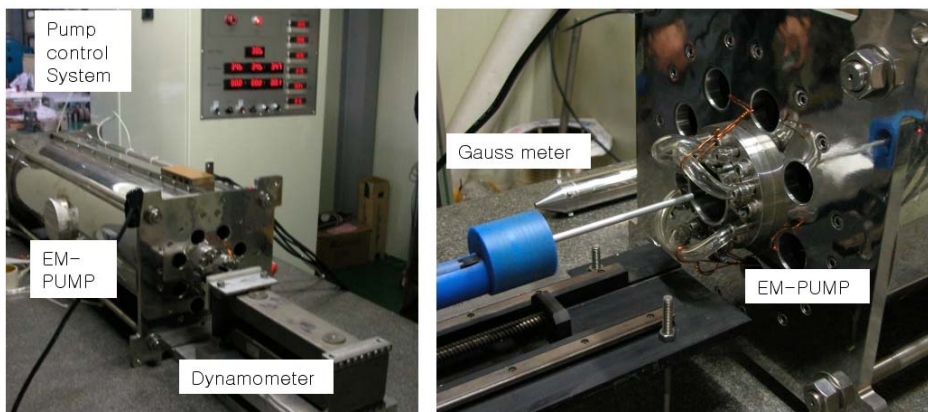
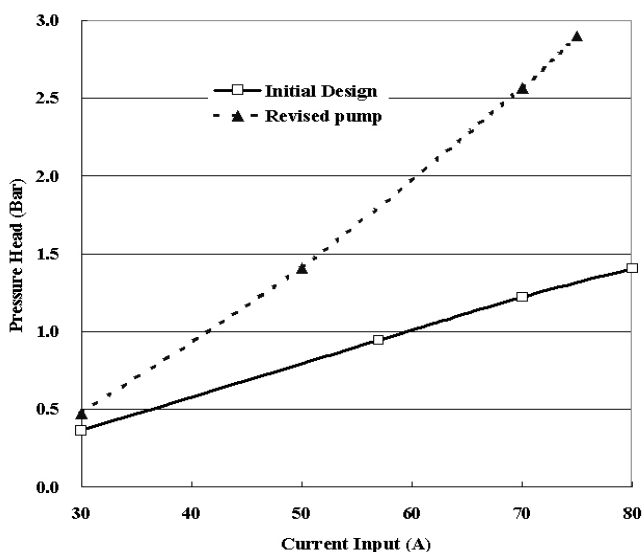


Figure 6 shows the performance of the EM pump. We calculated the pressure head from the measuring force by dividing the area of annular space between the outer duct and inner duct. The pressure head of the initial design was not enough to pump the LBE in the loop and thus we checked the magnetic field of annular space with the Gauss meter. The pressure head of the revised pump was

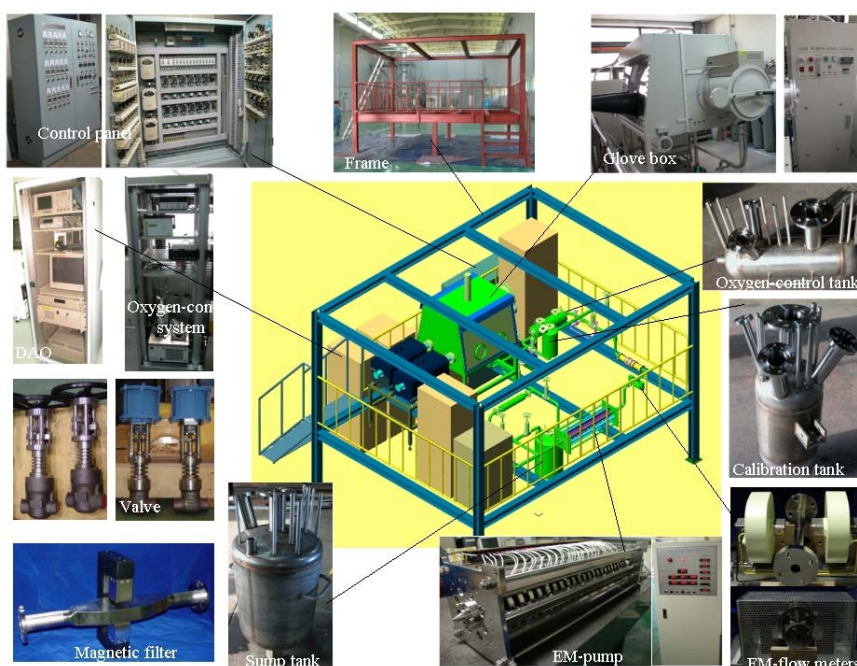
Figure 6. Pumping power of EM pump with current input



largely enhanced after changing the structure of the inner core and the inter-core gap between the inner core and outer core. From this test, we confirmed that the prototype EM pump could operate more than around 500 C and pumped the LBE more than 2.5 bar.

Figure 7 shows the schematics of the corrosion loop and its main components. Most of the components to be installed on the loop have already been manufactured, and a set-up process will be completed by the fall of 2004. The valve was specially manufactured for the LBE environment, which was considered for the temperature of seal and did not include any bellows.

Figure 7. State of the art of KAERI's corrosion loop installation



Conclusions

KAERI finished the set-up of the LBE static corrosion facility and started a static test for material screening and a systematic research to develop the measuring techniques for the control of oxygen concentration. KAERI completed the preliminary design of a dynamic corrosion loop on the basis of thermal and hydraulic experience of the sodium test and started a set-up process to construct the loop by the fall of 2004. From the EM pump test, we confirmed that the prototype EM pump could operate at more than around 500 C and the LBE pumped at a rate of more than 2.5 bar.

REFERENCES

- [1] Park, W-S., *et al.*, *Development of Nuclear Transmutation Technology*, KAERI report, KAERI/RR-1702/96 (1996).
- [2] Lai, G.Y., “High Temperature Corrosion of Engineering Alloys”, ASM Int., Materials Park, OH 44073 (1990).
- [3] Orlov, Y.I., *et al.*, “The Problems of Technology of the Heavy Liquid Metal Coolants (Lead-Bismuth, Lead)”, *Proc. of the Heavy Liquid Metal Coolants in Nuclear Technology*, Obninsk (1998).
- [4] Mueller, G., *et al.*, “Investigation on Oxygen Controlled Liquid Lead Corrosion of Surface Treated Steels”, *J. of Nuclear Materials*, 278, 85-95 (2000).
- [5] Shercliff, J.A., “The Theory of Electromagnetic Flow Measurement”, Cambridge University Press (1962).

TABLE OF CONTENTS

Foreword	3
Executive Summary.....	11
Welcome.....	15
<i>D-S. Yoon</i> Congratulatory Address	17
<i>I-S. Chang</i> Welcome Address	19
<i>G.H. Marcus</i> OECD Welcome	21
GENERAL SESSION: ACCELERATOR PROGRAMMES AND APPLICATIONS.....	23
<i>CHAIRS: B-H. CHOI, R. SHEFFIELD</i>	
<i>T. Mukaiyama</i> Background/Perspective.....	25
<i>M. Salvatores</i> Accelerator-driven Systems in Advanced Fuel Cycles	27
<i>S. Noguchi</i> Present Status of the J-PARC Accelerator Complex	37
<i>H. Takano</i> R&D of ADS in Japan.....	45
<i>R.W. Garnett, A.J. Jason</i> Los Alamos Perspective on High-intensity Accelerators.....	57
<i>J-M. Lagniel</i> French Accelerator Research for ADS Developments.....	69
<i>T-Y. Song, J-E. Cha, C-H. Cho, C-H. Cho, Y. Kim, B-O. Lee, B-S. Lee, W-S. Park, M-J. Shin</i> Hybrid Power Extraction Reactor (HYPER) Project	81

<i>V.P. Bhatnagar, S. Casalta, M. Hugon</i> Research and Development on Accelerator-driven Systems in the EURATOM 5 th and 6 th Framework Programmes.....	89
<i>S. Monti, L. Picardi, C. Rubbia, M. Salvatores, F. Troiani</i> Status of the TRADE Experiment.....	101
<i>P. D'hondt, B. Carlucci</i> The European Project PDS-XADS “Preliminary Design Studies of an Experimental Accelerator-driven System”.....	113
<i>F. Groeschel, A. Cadiou, C. Fazio, T. Kirchner, G. Laffont, K. Thomsen</i> Status of the MEGAPIE Project.....	125
<i>P. Pierini, L. Burgazzi</i> ADS Accelerator Reliability Activities in Europe	137
<i>W. Gudowski</i> ADS Neutronics	149
<i>P. Coddington</i> ADS Safety	151
<i>Y. Cho</i> Technological Aspects and Challenges for High-power Proton Accelerator-driven System Application.....	153
TECHNICAL SESSION I: ACCELERATOR RELIABILITY.....	163
<i>CHAIRS: A. MUELLER, P. PIERINI</i>	
<i>D. Vandeplasseche, Y. Jongen (for the PDS-XADS Working Package 3 Collaboration)</i> The PDS-XADS Reference Accelerator	165
<i>N. Ouchi, N. Akaoka, H. Asano, E. Chishiro, Y. Namekawa, H. Suzuki, T. Ueno, S. Noguchi, E. Kako, N. Ohuchi, K. Saito, T. Shishido, K. Tsuchiya, K. Ohkubo, M. Matsuoka, K. Sennyu, T. Murai, T. Ohtani, C. Tsukishima</i> Development of a Superconducting Proton Linac for ADS.....	175
<i>C. Miélot</i> Spoke Cavities: An Asset for the High Reliability of a Superconducting Accelerator; Studies and Test Results of a $\beta = 0.35$, Two-gap Prototype and its Power Coupler at IPN Orsay	185
<i>X.L. Guan, S.N. Fu, B.C. Cui, H.F. Ouyang, Z.H. Zhang, W.W. Xu, T.G. Xu</i> Chinese Status of HPPA Development	195

<i>J.L. Biarrotte, M. Novati, P. Pierini, H. Safa, D. Uriot</i> Beam Dynamics Studies for the Fault Tolerance Assessment of the PDS-XADS Linac	203
<i>P.A. Schmelzbach</i> High-energy Beat Transport Lines and Delivery System for Intense Proton Beams	215
<i>M. Tanigaki, K. Mishima, S. Shiroya, Y. Ishi, S. Fukumoto, S. Machida, Y. Mori, M. Inoue</i> Construction of a FFAG Complex for ADS Research in KURRI	217
<i>G. Ciavola, L. Celona, S. Gammino, L. Andò, M. Presti, A. Galatà, F. Chines, S. Passarello, XZh. Zhang, M. Winkler, R. Gobin, R. Ferdinand, J. Sherman</i> Improvement of Reliability of the TRASCO Intense Proton Source (TRIPS) at INFN-LNS	223
<i>R.W. Garnett, F.L. Krawczyk, G.H. Neuschaefer</i> An Improved Superconducting ADS Driver Linac Design.....	235
<i>A.P. Durkin, I.V. Shumakov, S.V. Vinogradov</i> Methods and Codes for Estimation of Tolerance in Reliable Radiation-free High-power Linac	245
<i>S. Henderson</i> Status of the Spallation Neutron Source Accelerator Complex	257
TECHNICAL SESSION II: TARGET, WINDOW AND COOLANT TECHNOLOGY.....	265
CHAIRS: X. CHENG, T-Y. SONG	
<i>Y. Kurata, K. Kikuchi, S. Saito, K. Kamata, T. Kitano, H. Oigawa</i> Research and Development on Lead-bismuth Technology for Accelerator-driven Transmutation System at JAERI	267
<i>P. Michelato, E. Bari, E. Cavaliere, L. Monaco, D. Sertore, A. Bonucci, R. Giannantonio, L. Cinotti, P. Turroni</i> Vacuum Gas Dynamics Investigation and Experimental Results on the TRASCO ADS Windowless Interface	279
<i>J-E. Cha, C-H. Cho, T-Y. Song</i> Corrosion Tests in the Static Condition and Installation of Corrosion Loop at KAERI for Lead-bismuth Eutectic	291
<i>P. Schuurmans, P. Kupschus, A. Verstrepen, J. Cools, H. Ait Abderrahim</i> The Vacuum Interface Compatibility Experiment (VICE) Supporting the MYRRHA Windowless Target Design	301

<i>C-H. Cho, Y. Kim, T-Y. Song</i> Introduction of a Dual Injection Tube for the Design of a 20 MW Lead-bismuth Target System.....	313
<i>H. Oigawa, K. Tsujimoto, K. Kikuchi, Y. Kurata, T. Sasa, M. Umeno, K. Nishihara, S. Saito, M. Mizumoto, H. Takano, K. Nakai, A. Iwata</i> Design Study Around Beam Window of ADS.....	325
<i>S. Fan, W. Luo, F. Yan, H. Zhang, Z. Zhao</i> Primary Isotopic Yields for MSDM Calculations of Spallation Reactions on ²⁸⁰ Pb with Proton Energy of 1 GeV.....	335
<i>N. Tak, H-J. Neitzel, X. Cheng</i> CFD Analysis on the Active Part of Window Target Unit for LBE-cooled XADS.....	343
<i>T. Sawada, M. Orito, H. Kobayashi, T. Sasa, V. Artisyuk</i> Optimisation of a Code to Improve Spallation Yield Predictions in an ADS Target System.....	355
TECHNICAL SESSION III: SUBCRITICAL SYSTEM DESIGN AND ADS SIMULATIONS.....	363
<i>CHAIRS: W. GUDOWSKI, H. OIGAWA</i>	
<i>T. Misawa, H. Unesaki, C.H. Pyeon, C. Ichihara, S. Shiroya</i> Research on the Accelerator-driven Subcritical Reactor at the Kyoto University Critical Assembly (KUCA) with an FFAG Proton Accelerator.....	365
<i>K. Nishihara, K. Tsujimoto, H. Oigawa</i> Improvement of Burn-up Swing for an Accelerator-driven System	373
<i>S. Monti, L. Picardi, C. Ronsivalle, C. Rubbia, F. Troiani</i> Status of the Conceptual Design of an Accelerator and Beam Transport Line for Trade.....	383
<i>A.M. Degtyarev, A.K. Kalugin, L.I. Ponomarev</i> Estimation of some Characteristics of the Cascade Subcritical Molten Salt Reactor (CSMSR).....	393
<i>F. Roelofs, E. Komen, K. Van Tichelen, P. Kupschus, H. Ait Abderrahim</i> CFD Analysis of the Heavy Liquid Metal Flow Field in the MYRRHA Pool.....	401
<i>A. D'Angelo, B. Arien, V. Sobolev, G. Van den Eynde, H. Ait Abderrahim, F. Gabrielli</i> Results of the Second Phase of Calculations Relevant to the WPPT Benchmark on Beam Interruptions	411

TECHNICAL SESSION IV: SAFETY AND CONTROL OF ADS 423

CHAIRS: J-M. LAGNIEL, P. CODDINGTON

*P. Coddington, K. Mikityuk, M. Schikorr, W. Maschek,
R. Sehgal, J. Champigny, L. Mansani, P. Meloni, H. Wider*
Safety Analysis of the EU PDS-XADS Designs..... 425

*X-N. Chen, T. Suzuki, A. Rineiski, C. Matzerath-Boccaccini,
E. Wiegner, W. Maschek*
Comparative Transient Analyses of Accelerator-driven Systems
with Mixed Oxide and Advanced Fertile-free Fuels 439

P. Coddington, K. Mikityuk, R. Chawla
Comparative Transient Analysis of Pb/Bi
and Gas-cooled XADS Concepts 453

B.R. Sehgal, W.M. Ma, A. Karbojian
Thermal-hydraulic Experiments on the TALL LBE Test Facility 465

K. Nishihara, H. Oigawa
Analysis of Lead-bismuth Eutectic Flowing into Beam Duct..... 477

P.M. Bokov, D. Ridikas, I.S. Slessarev
On the Supplementary Feedback Effect Specific
for Accelerator-coupled Systems (ACS)..... 485

W. Haeck, H. Ait Abderrahim, C. Wagemans
 K_{eff} and K_s Burn-up Swing Compensation in MYRRHA 495

TECHNICAL SESSION V: ADS EXPERIMENTS AND TEST FACILITIES 505

CHAIRS: P. D'HONDT, V. BHATNAGAR

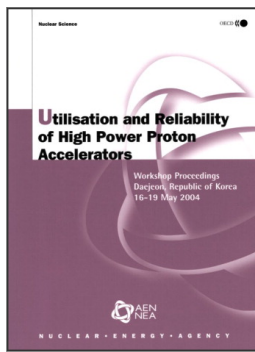
*H. Oigawa, T. Sasa, K. Kikuchi, K. Nishihara, Y. Kurata, M. Umeno,
K. Tsujimoto, S. Saito, M. Futakawa, M. Mizumoto, H. Takano*
Concept of Transmutation Experimental Facility 507

M. Hron, M. Mikisek, I. Peka, P. Hosnedl
Experimental Verification of Selected Transmutation Technology and Materials
for Basic Components of a Demonstration Transmuter with Liquid Fuel
Based on Molten Fluorides (Development of New Technologies for
Nuclear Incineration of PWR Spent Fuel in the Czech Republic) 519

Y. Kim, T-Y. Song
Application of the HYPER System to the DUPIC Fuel Cycle..... 529

M. Plaschy, S. Pelloni, P. Coddington, R. Chawla, G. Rimpault, F. Mellier
Numerical Comparisons Between Neutronic Characteristics of MUSE4
Configurations and XADS-type Models 539

<i>B-S. Lee, Y. Kim, J-H. Lee, T-Y. Song</i> Thermal Stability of the U-Zr Fuel and its Interfacial Reaction with Lead	549
SUMMARIES OF TECHNICAL SESSIONS	557
<i>CHAIRS: R. SHEFFIELD, B-H. CHOI</i>	
<i>Chairs: A.C. Mueller, P. Pierini</i> Summary of Technical Session I: Accelerator Reliability	559
<i>Chairs: X. Cheng, T-Y. Song</i> Summary of Technical Session II: Target, Window and Coolant Technology	565
<i>Chairs: W. Gudowski, H. Oigawa</i> Summary of Technical Session III: Subcritical System Design and ADS Simulations.....	571
<i>Chairs: J-M. Lagniel, P. Coddington</i> Summary of Technical Session IV: Safety and Control of ADS	575
<i>Chairs: P. D'hondt, V. Bhatagnar</i> Summary of Technical Session V: ADS Experiments and Test Facilities.....	577
SUMMARIES OF WORKING GROUP DISCUSSION SESSIONS	581
<i>CHAIRS: R. SHEFFIELD, B-H. CHOI</i>	
<i>Chair: P.K. Sigg</i> Summary of Working Group Discussion on Accelerators.....	583
<i>Chair: W. Gudowski</i> Summary of Working Group Discussion on Subcritical Systems and Interface Engineering	587
<i>Chair: P. Coddington</i> Summary of Working Group Discussion on Safety and Control of ADS.....	591
<i>Annex 1: List of workshop organisers</i>	<i>595</i>
<i>Annex 2: List of participants.....</i>	<i>597</i>



From:

Utilisation and Reliability of High Power Proton Accelerators

Workshop Proceedings, Daejeon, Republic of Korea, 16-19 May 2004

Access the complete publication at:

<https://doi.org/10.1787/9789264013810-en>

Please cite this chapter as:

Cha, J.-E., Chung-Ho Cho and T.-Y. Song (2006), "Corrosion Tests in the Static Condition and Installation of Corrosion Loop at KAERI for Lead-Bismuth Eutectic", in OECD/Nuclear Energy Agency, *Utilisation and Reliability of High Power Proton Accelerators: Workshop Proceedings, Daejeon, Republic of Korea, 16-19 May 2004*, OECD Publishing, Paris.

DOI: <https://doi.org/10.1787/9789264013810-31-en>

This work is published under the responsibility of the Secretary-General of the OECD. The opinions expressed and arguments employed herein do not necessarily reflect the official views of OECD member countries.

This document and any map included herein are without prejudice to the status of or sovereignty over any territory, to the delimitation of international frontiers and boundaries and to the name of any territory, city or area.

You can copy, download or print OECD content for your own use, and you can include excerpts from OECD publications, databases and multimedia products in your own documents, presentations, blogs, websites and teaching materials, provided that suitable acknowledgment of OECD as source and copyright owner is given. All requests for public or commercial use and translation rights should be submitted to rights@oecd.org. Requests for permission to photocopy portions of this material for public or commercial use shall be addressed directly to the Copyright Clearance Center (CCC) at info@copyright.com or the Centre français d'exploitation du droit de copie (CFC) at contact@cfcopies.com.